Korean J. Chem. Eng., **17**(3), 351-356 (2000)

Simulation Studies of Nearest-Neighbor Distribution Functions and Related Structural Properties for Hard-Sphere Systems

Soong-Hyuck Suh†, Woong-Ki Min, Viorel Chihaia, Jae-Wook Lee* and Soon-Chul Kim**

Department of Chemical Engineering, Keimyung University, Taegu 704-701, Korea
*Department of Chemical Engineering, Seonam University, Namwon 590-170, Korea
**Department of Physics, Andong National University, Andong 760-749, Korea
(*Received 17 January 2000 • accepted 19 February 2000)*

Abstract−Molecular dynamics simulations have been carried out to investigate nearest-neighbor distribution functions and closely related quantities for the system of hard-spheres. The nearest-neighbor distribution function and the exclusion probability function were computed to examine the density dependence on the structural 'void' and 'particle' properties. Simulation results were used to access the applicabilities of various theoretical predictions based on the scaled-particle theory, the Percus-Yevick equation, and the Carnahan-Starling approximation. For lower density systems the three different approximations give the nearest-neighbor distribution functions which are very close to one another and also to the resulting simulation data. Among those theoretical predictions, the Carnahan-Starling approximation gives remarkably good agreement with the simulation data even for higher density systems. Also calculated is the *n*th moment of the nearest-neighbor distribution functions, in which the corresponding length scale is directly related to the measurement of the characteristic pore-size distribution.

Key words: Molecular Dynamics Simulation, Nearest-Neighbor Distribution, Exclusion Probability Function

INTRODUCTION

Two-phase random media, such as composite materials, amorphous solids and porous media [Alder, 1992; Dullien, 1992], are of great fundamental as well as practical importance to engineers and scientists working in many areas such as heterogeneous catalysis, membrane separation, effective conductivity and diffusion of molecules in micropores. The structural or morphological information can be ascertained either theoretically or experimentally. From the theoretical point of view, it is desired to determine the static and dynamic properties of two-phase disordered media to obtain the optimized microstructures under equilibrium conditions. Experimentally, it has also become possible to obtain two- and three-dimensional phase information by using a variety of experimental techniques. An example is the experimental microtomographic methods together with theoretical approaches to study the structural and transport properties of a porous magnetic gel [Rintoul et al., 1996].

The detailed structural functions and their closely related quantities can be evaluated exactly only for a few cases including the one-dimensional system of hard-rods. For two or more dimensional cases such as the systems of hard-discs and hard-spheres, however, complete morphological information is not known analytically since an infinite set of statistical functions that characterize related microstructures are required to be determined. Recently, Torquato and his co-workers [Torquato et al., 1990] derived an integral representation of *N*-point distribution functions and applied them for model interaction systems [Torquato and Avellaneda, 1991; Quintanilla and Torquato, 1997]. By using the lower-order correlation functional information, they investigated upper or lower bounds on many of the properties of such higher dimensional systems. Reliable and unambiguous results have become increasingly necessary to eliminate any underlying uncertainties involved in these theoretical predictions. Consequently, computer simulations have proven to be an extremely useful diagnostic tool for investigating such systems [Allen and Tildesley, 1987; Gubbins and Quirke, 1997].

In this study computer simulations via the molecular dynamics method for hard-spheres systems have been carried out to access the applicabilities of various theoretical expressions appearing in the literature, namely, the scaled-particle, Percus-Yevick and Carnahan-Starling approximations. Such information including the nearest-neighbor distribution function and the exclusion probability function can be used to investigate not only the qualitative characterization of the microstructure but also the dynamic transport problem in the model random media. The selected examples for dynamic properties include the application of Knudsen diffusion in fully or partially overlapping porous media [MacElroy, 1996; Suh et al., 1999] and membrane gas separation [Aoki et al., 1996]. Many of the results obtained in this work can also be easily extended to random model pore systems, e.g., the penetrable-concentric-shell model pore [Suh et al., 1999], in which the solid matrix is represented as assemblies of penetrable spheres randomly distributed in the pore phase.

NEAREST-NEIGHBOR DISTRIBUTION FUNCTIONS AND RELATED QUANTITIES

Torquato et al. [1990] first introduced the so-called nearest-neighbor distribution functions and their related quantities for

†To whom correspondence should be addressed.
E-mail: shsuh@kmucc.keimyung.ac.kr

the system of *N* identical hard-spheres of diameter σ according to the *N*-point probability density function. They defined the two different types of probability functions of $H_V(r)$ and $H_P(r)$, which are referred to as the 'void' and 'particle' nearest-neighbor distribution functions, respectively. $H_V(r)$ provides a measure of the probability associated with finding the nearest particle at a distance r from any arbitrary point in the system. Similarly, $H_P(r)$ represents the probability of finding the nearest particle at a distance r from an actual particle at the origin. For statistically homogeneous media, as demonstrated in their work, one can relate the nearest-neighbor distribution functions to the radial distribution functions. Note that H_V and H_P are the normalized probability functions and have dimensions of inverse length.

It follows that the 'void' and 'particle' exclusion probability functions, $E_V(r)$ and $E_P(r)$, are defined by means of the nearest-neighbor distribution functions, i.e.,

$$E_V(r)=1-\int_0^r H_V(r)dr \tag{1}$$

and

$$E_P(r)=1-\int_0^r H_P(r)dr \tag{2}$$

Differentiating Eqs. (1) and (2) with respect to r, we have simple relationships between the exclusion and nearest probabilities functions as

$$H_V(r)=-\frac{dE_V(r)}{dr} \tag{3}$$

and

$$H_P(r)=-\frac{dE_P(r)}{dr} \tag{4}$$

From the physical definition for rigid hard-sphere systems, a spherical cavity of radius r and its volume $4\pi r^3/3$ can contain at most one particle center if $0\le r\le\sigma/2$. Thus, for $0\le r\le\sigma/2$, the exclusion probability $E_V(r)$ can be given by

$$E_V(r)=1-\frac{4\pi r^3}{3}\rho, \quad \text{if } 0\le r\le\sigma/2 \tag{5}$$

and, from Eq. (3), one may also have

$$H_V(r)=4\pi r^2\rho, \quad \text{if } 0\le r\le\sigma/2 \tag{6}$$

where ρ is the particle number density.

Furthermore, in the case of the 'particle' problems, spheres are totally impenetrable and one sphere excludes another from occupying the same place. For the range of $0\le r\le\sigma$, one can state the exact relations that

$$E_P(r)=1, \quad \text{if } 0\le r\le\sigma \tag{7}$$

$$H_P(r)=0, \quad \text{if } 0\le r\le\sigma \tag{8}$$

Except for one-dimensional hard-rod systems, it is not possible to evaluate the nearest-neighbor distribution function for higher dimensions because the *N*-point probability density functions are not exactly known. As derived in the previous work [Torquato et al., 1990], three different approximation schemes were considered, namely, scaled-particle, Percus-Yevick and Carnahan-Starling approximations [Reed and Gubbins, 1973; Hansen and McDonald, 1976].

Using the scaled-particle theory, the analytical expression for the 'void' and 'particle' quantities can be written as

$$E_V(x)=(1-\eta)\exp[-\eta(8ax^3+12bx^2+24cx+d)], \quad \text{if } x(=r/\sigma)\ge0.5 \tag{9}$$

$$E_P(x)=\exp[-\eta\{8a(x^3-1)+12b(x^2-1)+24c(x-1)\}], \quad \text{if } x(=r/\sigma)\ge1 \tag{10}$$

where

$$a(\eta)=\frac{1+\eta+\eta^2}{(1-\eta)^3} \tag{11}$$

$$b(\eta)=\frac{-3\eta(1+\eta)}{2(1-\eta)^3} \tag{12}$$

$$c(\eta)=\frac{3\eta^2}{4(1-\eta)^3} \tag{13}$$

$$d(\eta)=\frac{-11\eta^2+7\eta-2}{2(1-\eta)^3} \tag{14}$$

and

$$\eta=\frac{\pi}{6}\rho\sigma^3 \tag{15}$$

is a reduced packing density that is identical to the packing fraction of impenetrable hard-spheres.

The 'void' exclusion distribution $E_V(r)$ is directly related to the probability of inserting a test particle into the system of hard-spheres. This quantity can be evaluated from radial distribution functions between a single test particle (at infinite dilution) of radius $r-\sigma/2$ and hard-spheres of diameter σ. If one considers the Percus-Yevick solution for such a special binary mixture of hard-spheres, then

$$E_V(x)=(1-\eta)\exp\left[\frac{-\eta}{(1-\eta)^2}\{8(1+2\eta)x^3-18\eta x^2+2.5\eta-1\}\right], \quad \text{if } x(=r/\sigma)\ge0.5 \tag{16}$$

$$E_P(x)=\exp\left[\frac{-\eta}{(1-\eta)^2}\{8(1+2\eta)(x^3-1)-18\eta(x^2-1)\}\right], \quad \text{if } x(=r/\sigma)\ge1 \tag{17}$$

Guided by computer simulation data, Carnahan and Starling devised a simple but very accurate hard-sphere equation of state and related thermodynamic properties. The Carnahan-Starling equation of state can be recovered by adding the two Percus-Yevick equations of state, i.e., the compressibility and the virial equation of state with weights of two-third and one-third, respectively. By means of the Carnahan-Starling approximation, we have

$$E_V(x)=(1-\eta)\exp[-\eta(8ex^3+12fx^2+24gx+h)], \quad \text{if } x(=r/\sigma)\ge0.5 \tag{18}$$

$$E_P(x)=\exp[-\eta\{8e(x^3-1)+12f(x^2-1)+24g(x-1)\}], \quad \text{if } x(=r/\sigma)\ge1 \tag{19}$$

where

$$e(\eta)=\frac{1+\eta}{(1-\eta)^3} \tag{20}$$

$$f(\eta)=\frac{-\eta(3+\eta)}{2(1-\eta)^3} \tag{21}$$

$$g(\eta)=\frac{\eta^2}{2(1-\eta)^3} \tag{22}$$

$$h(\eta)=\frac{-9\eta^2+7\eta-2}{2(1-\eta)^3} \tag{23}$$

By the relationships between the exclusion and nearest probabilities defined in Eqs. (3) and (4), one can straightforwardly calculate $H_V(r)$ and $H_P(r)$ for the aforementioned approximations. Although the 'void' and 'particle' quantities are not the same for $r<\sigma$, they are related to one another for the range of $r\geq\sigma$

$$E_P(r)=\frac{E_V(r)}{E_V(\sigma)} \quad \text{for } r\geq\sigma \tag{24}$$

and

$$H_P(r)=\frac{H_V(r)}{E_V(\sigma)} \quad \text{for } r\geq\sigma \tag{25}$$

In the limit of $\eta\rightarrow 0$, it is clear that $H_V(r)=H_P(r)$.

RESULTS AND DISCUSSION

As described in the previous section, the three approximations based on different statistical thermodynamic approaches were made to determine the nearest-neighbor distribution functions and its related quantities. It should be noted that the introduction of simplifying approximations in those equations is required only because of the mathematical intractability of the formal equation of the *N*-point probability density function. One of the interesting questions investigated in this study is related to the applicabilities of such theoretical approximations. This can be directly tested by comparing against computer simulation results, and molecular-based simulations used in this way can provide essentially exact data for precisely defined model systems.

In this regard we carried out molecular dynamics (MD) simulations using the hard-sphere dynamics algorithm introduced in the pioneering work of Alder and Wainwright [1959]. In this method, all possible collisions were evaluated and scanned to determine the minimum collision time. Then the particles were moved at constant velocity during the time for the first pair to collide. Post-collisional velocities for a colliding pair were assigned according to elastic collision dynamics and new collision times were reevaluated for the particles involved in possible collisions. This procedure is repeated as many times as is desired. The conventional periodic boundary conditions were applied in a cubic fundamental cell to approximate an infinite system. At lower densities of $\eta\leq 0.35$, the initial configurations were generated by randomly inserting spheres to assist in the equilibration of the system. For higher densities, the initial positions were taken from the regular sites on a face-centered-cubic lattice. The initial velocities of particles were assigned from the equilibrium Maxwell-Boltzmann distribution function. The MD calculations

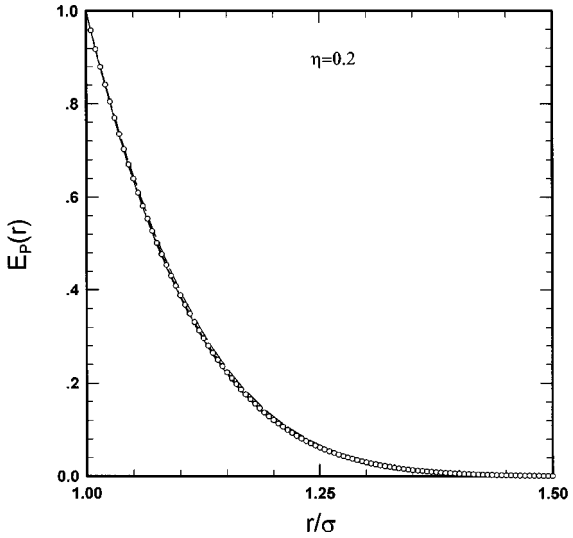

Fig. 1. The 'particle' exclusion probability function $E_P(r)$ as a function of the reduced separation distance r/σ for η= 0.2. Theoretical predictions based on the scaled-particle, Percus-Yevick, Carnahan-Starling approximations are represented as the solid, dotted and chain-dotted curves, respectively. Also shown as the open circles correspond to the MD simulation data.

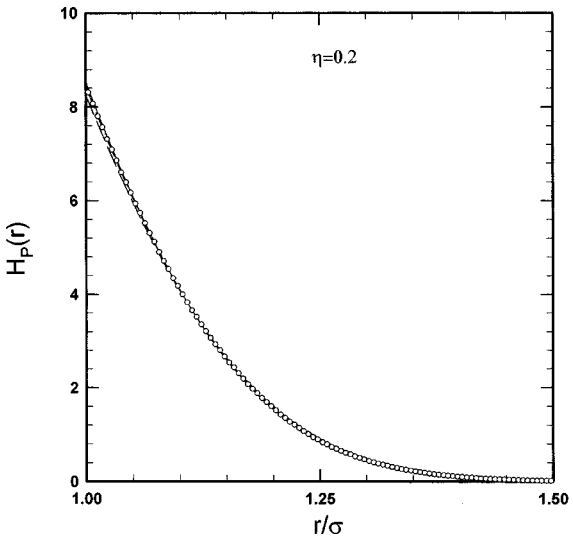

Fig. 2. The 'particle' nearest-neighbor distribution function H_P (r) as a function of the reduced separation distance r/σ for η=0.2. Lines and symbols are the same as in Fig. 1.

were performed for the system containing 500 hard-spheres. Starting configurations were aged, or equilibrated, during 10^5 collision steps before data were accumulated and the resulting ensemble averages for a given condition were obtained from the final 10^7 collision steps.

In Fig. 1 through Fig. 4, we have plotted the MD simulation data together with the aforementioned theoretical predictions for the 'particle' exclusion probability functions, $E_P(r)$, and the 'particle' nearest-neighbor distribution functions, $H_P(r)$, as a function of r in units of the sphere diameter, σ. The open circles in these figures correspond to the MD data, and the solid, dotted and

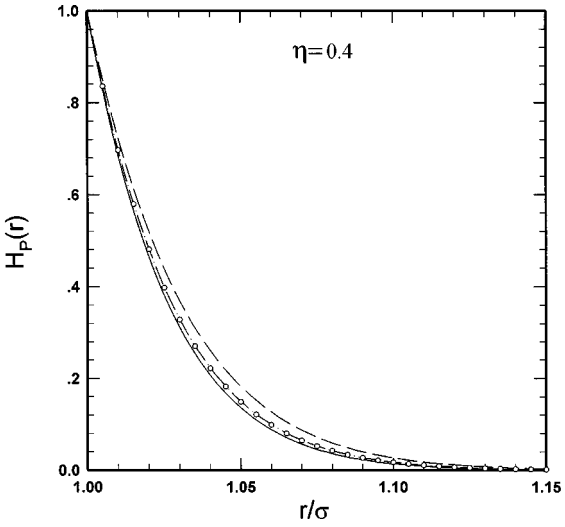

Fig. 3. The 'particle' exclusion probability function $E_P(r)$ as a function of the reduced separation distance r/σ for η= 0.4. Lines and symbols are the same as in Fig. 1.

chain-dotted curves to three different theoretical predictions based on scaled-particle, Percus-Yevick, and Carnahan-Starling approximations, respectively. For the case of low density (η= 0.2), as displayed in Figs. 1 and 2, three approximations give the values of $E_P(r)$ and $H_P(r)$ which are very close to one another and also to the MD data. The good agreement with the resulting simulation data apparently indicates the support to theoretical predictions.

Figs. 3 and 4, respectively, depict $E_P(r)$ and $H_P(r)$ for the high density of η=0.4. Although the general agreement is good, more profound deviations, compared with the lower density system in Figs. 1 and 2, are found between the approximations themselves and between the approximations and the MD data. As can be seen in these figures, the functions of $E_P(r)$ and $H_P(r)$ decrease with increasing separation distance r because the probability of finding a nearest-neighbor particle center reaches its maximum at $r=\sigma$ and diminishes monotonically for $r\geq\sigma$. It should be noted that the radial distribution function for the corresponding hard-sphere systems, which is related to the probability of finding particle at a distance between r and r+ dr, does not behave monotonically but does exhibit oscillatory behavior even at the moderate density regime [Hansen and McDonald, 1976].

One of the interesting features illustrated in Fig. 4 is that theoretical results obtained from the Percus-Yevick approximation can either underestimate or overestimate the values of $H_P(r)$ depending on the separation distance r. The Percus-Yevick solution for the radial distribution function of hard-sphere systems is known to be more inaccurate with increasing the particle density. For high density systems, the value at contact is too low and the amplitude of the oscillations decreases too slowly with increasing distance [Reed and Gubbins, 1973]. The low contact value leads to the underestimation of $H_P(r)$ near the contact distance, while a consequence of mismatching oscillation phase results in the overestimation of $H_P(r)$ with farther extending the particle separation. On the contrary, as shown in Fig. 4, the scaled-particle theory gives higher values of $H_P(r)$ near the contact distance and slightly lower values for $r/\sigma\geq$ 1.03. Among three theoretical equations, the Carnahan-Starling approximation is shown to be the best and in excellent agreement with the simulation results.

In Figs. 5 and 6, respectively, we have plotted the 'void' exclusion probability functions, $E_V(r)$, and the 'void' nearest-neighbor distribution functions, $H_V(r)$, for a few selected runs of η=0.2, η=0.3 and η=0.4 to illustrate the manner in which the functions of $E_V(r)$ and $H_V(r)$ change with increasing density. In evaluating those functions in the MD computations, 10×10× 10 lattice points are thrown into the fundamental cubic cell with the equal time interval. For each lattice point, the smallest distance from the point to the nearest particle is calculated and

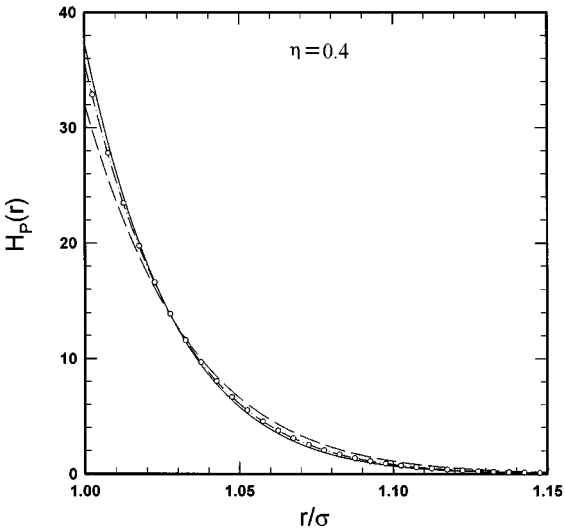

Fig. 4. The 'particle' nearest-neighbor distribution function H_P (r) as a function of the reduced separation distance r/σ for η=0.4. Lines and symbols are the same as in Fig. 1.

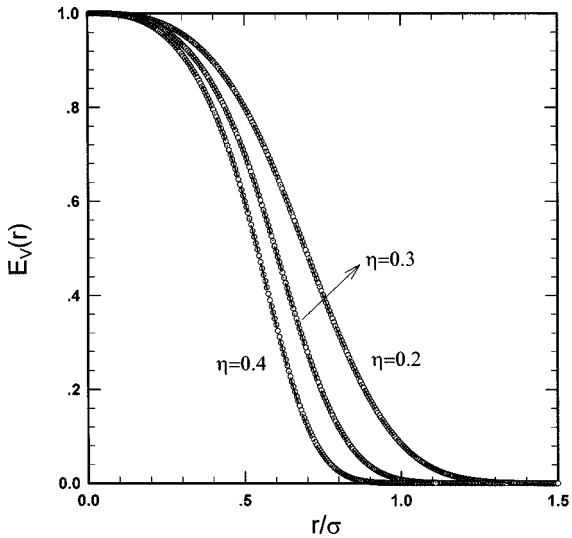

Fig. 5. The 'void' exclusion probability function $E_V(r)$ as a function of the reduced separation distance r/σ for η= 0.2, η=0.3 and η=0.4. The open circles and the chaindotted curves correspond to the MD simulation data and the Carnahan-Starling approximation, respectively.

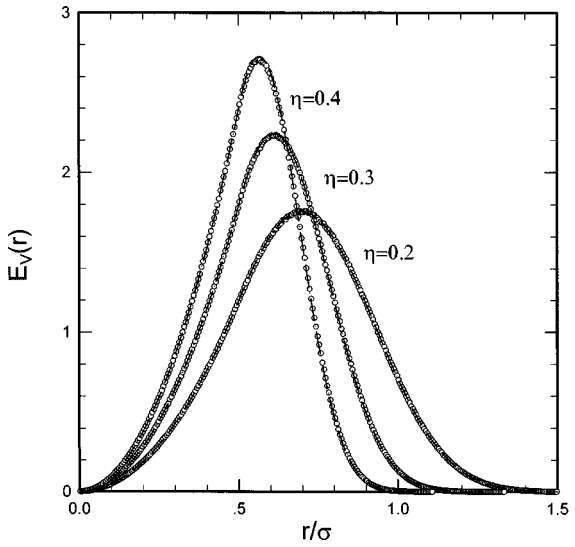

Fig. 6. The 'void' nearest-neighbor distribution function $H_V(r)$ as a function of the reduced separation distance r/σ for η=0.2, η=0.3 and η=0.4. Lines and symbols are the same as in Fig. 5.

the quantities of $E_V(r)$ and $H_V(r)$ are determined by binning these distances. In the end, all counters are divided by the total sampling number.

As shown in Figs. 5 and 6 for the 'void' properties, the theoretical results obtained form the Carnahan-Starling approximation are again seen to be in remarkably good agreement with the MD simulation data. The quantity $E_V(r)$ has the interpretation of the volume fraction of space occupied by a system of possibly overlapping spheres of radius r centered at each of the actual sphere centers. Similarly, $H_V(r)$, which is identical to the one defined in the scaled-particle theory, can be interpreted as being the interfacial area per unit volume of a system of possibly overlapping spheres of radius r centered at each of the actual sphere centers. The quality of our MD sampling employed here was confirmed by the fact that the resulting simulation values for $E_V(r)$ at $r=\sigma/2$ were very close to the expected value of $E_V(\sigma/2)=1-\eta$. When $r\geq\sigma/2$, a spherical cavity centered in the void region, i.e., the region exterior to the spheres, and the measurement $H_V(r)/(1-\eta)$ in this range is related to the pore-size distribution function. The pore-size distribution deduced from $H_V(r)$ in Fig. 6 indicates much narrower distributions for the higher density system (η=0.4) than those for the lower one (η=0.2), as one may expect.

Finally, we have calculated the nth moment of $H_V(r)$ and $H_P(r)$, which can be defined as

$$l_V^{(n)}=\int_0^\infty r^n H_V(r)dr \tag{26}$$

$$l_P^{(n)}=\int_0^\infty r^n H_P(r)dr \tag{27}$$

or, using the integration by parts,

$$l_V^{(n)}=n\int_0^\infty r^{n-1}E_V(r)dr \tag{28}$$

$$l_P^{(n)}=n\int_0^\infty r^{n-1}E_P(r)dr$$

$$=\sigma^n+n\int_\sigma^\infty r^{n-1}E_P(r)dr \tag{29}$$

Table 1. Molecular dynamics simulation data for the nth moment of the 'void' and the 'particle' properties, $l_V^{(n)}$ and $l_P^{(n)}$

η	$l_V^{(1)}/\sigma$	$l_V^{(2)}/\sigma^2$	$l_V^{(3)}/\sigma^3$	$l_P^{(1)}/\sigma$	$l_P^{(2)}/\sigma^2$	$l_P^{(3)}/\sigma^3$
0.15	0.77305	0.66401	0.61697	1.1419	1.3176	1.5378
0.20	0.69130	0.52792	0.43405	1.0974	1.2112	1.3453
0.25	0.63342	0.44090	0.32895	1.0691	1.1467	1.2343
0.30	0.58963	0.38028	0.26180	1.0499	1.1042	1.1637
0.35	0.55498	0.33547	0.21563	1.0362	1.0748	1.1161
0.40	0.52668	0.30105	0.18236	1.0262	1.0537	1.0826
0.45	0.50317	0.27388	0.15748	1.0189	1.0384	1.0586

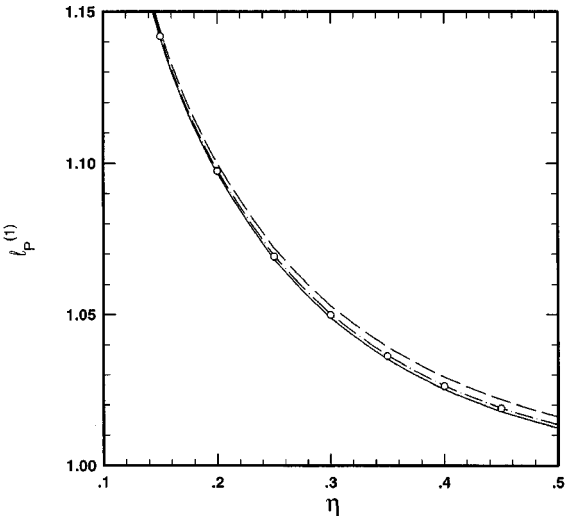

Fig. 7. The 1st moment (mean) of the 'particle' nearest-neighbor distribution function $l_P^{(1)}$ as a function of η. Lines and symbols are the same as in Fig. 1.

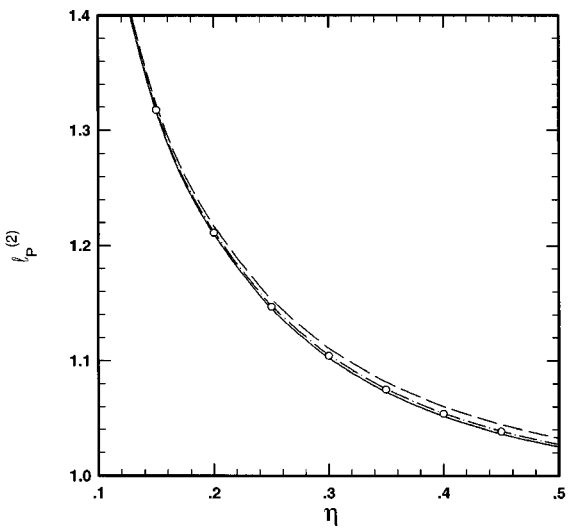

Fig. 8. The 2nd moment (variance) of the 'particle' nearest-neighbor distribution function $l_P^{(2)}$ as a function of η. Lines and symbols are the same as in Fig. 1.

In Table 1 the MD simulation results for $l_V^{(n)}$ and $l_P^{(n)}$ up to the third moment are presented to investigate the density dependencies on the pore geometries. The corresponding length scale

of $l_V^{(n)}$ and $l_P^{(n)}$ is directly related to the measurement of the characteristic pore-size distribution. For instance, the 1st and the 2nd moment of $l_P^{(n)}$ are the mean and the variation of nearest-neighbor distance, respectively. In Figs. 7 and 8 we illustrate the MD data for $l_P^{(1)}$ and $l_P^{(2)}$ together with the theoretical results determined from the three different approximations. Theoretical values from Eqs. (26) through (29) were calculated by numerical integration using the trapezoidal rule with the integration step of $10^{-4}\,\sigma$. As can be seen in these figures, these approximations are in reasonable qualitative agreement with simulation results over most of the range of the densities investigated in this work. In the cases of the scaled-particle and the Percus-Yevick approximations, the discrepancy is gradually amplified with increasing densities. As observed in the 'void' and 'particle' probability functions, the Carnahan-Starling approximation again yields the best result and the scaled-particle theory gives the next best agreement compared to our MD simulation data.

CONCLUSION

In the present work, we have reported preliminary simulation results via the molecular dynamics simulation method to investigate nearest-neighbor distribution functions and their related structural properties for hard-sphere systems. The 'void' and the 'particle' properties such as nearest-neighbor distribution functions and exclusion probability functions were calculated to examine the density dependence over a wide range of reduced packing densities. Our simulation results were used to access the applicabilities of various theoretical predictions appearing in the literature including the scaled-particle theory, the Percus-Yevick equation, and the Carnahan-Starling approximation. For lower density systems these three different approximations give the nearest-neighbor distribution functions which are very close to one another and to the resulting MD simulation data. In the cases of the scaled-particle and the Percus-Yevick approximations, the discrepancy is gradually amplified with increasing densities. As has been observed for the equation of state of hard-sphere systems, the Carnahan-Starling approximation, in comparison with MD simulation data, has proven to be successful both qualitatively and quantitatively in predicting the nearest-neighbor distribution functions over the entire ranges of density conditions investigated in this work. Also calculated is the nth moment of nearest-neighbor distribution functions, in which the corresponding length scale is directly related to the measurement of the characteristic pore-size distribution. The density dependencies on the pore-size characteristics would be very useful in gaining a better understanding of how effectively the modification of particle packing densities influences random pore geometries at the molecular level.

ACKNOWLEDGEMENT

This research is financially supported by the Korea Science and Engineering Foundation (981-1102-005-2) and the BK21 project.

REFERENCES

Alder, B. J. and Wainwright, T. E., "Studies in Molecular Dynamics. I. General Method," *J. Chem. Phys.*, **31**, 459 (1959).

Alder, P. M., "Porous Media: Geometry and Transport," Butterworth-Heinemann, Boston (1992).

Allen, M. P. and Tildesley, D. J., "Computer Simulation of Liquids," Clarendon, Oxford (1987).

Aoki, K., Yokoyama, S., Kusakabe, K. and Morooka, S., "Preparation of Supported Palladium Membrane and Separation of Hydrogen," *Korean J. Chem. Eng*., **13**, 530 (1996).

Dullien, F. A. L., "Porous Media: Fluid Transport and Pore Structure," Academic, New York (1992).

Gubbins, K. E. and Quirke, V., "Molecular Simulation and Industrial Applications: Methods, Examples and Prospects," Gordon and Breach, London (1997).

Hansen, J. P. and McDonald, I. R., "Theory of Simple Liquids," Academic, New York (1976).

MacElroy, J. M. D., "Diffusion in Polymers," Neogi, P., ed., Marcel Dekker, New York (1996).

Quintanilla, J. and Torquato, S., "Microstructure Functions for a Model of Statistically Inhomogeneous Random Media," *Phys. Rev. E*, **55**, 1558 (1997).

Reed, T. M. and Gubbins, K. E., "Applied Statistical Mechanics," McGraw-Hill, New York (1973).

Rintoul, M. D., Torquato, S., Yeong, C., Keane, D. T., Erramili, S., Jun, Y. N. and Dabbs, D. M., "Structure and Transport Properties of a Porous Magnetic Gel Via X-Ray Microtomography," *Phys. Rev. E*, **54**, 2663 (1996).

Suh, S.-H., Min, W.-K. and Kim, S.-C., "Molecular Simulation Studies for Knudsen Diffusion in the Overlapping Sphere Pore Model," *HWAHAK KONGHAK*, **37**, 557 (1999).

Suh, S.-H., Min, W.-K. and MacElroy, J. M. D., "Simulation Studies for Porosity and Specific Surface Area in the Penetrable-Concentric-Shell Model Pore," *Bull. Korean Chem. Soc.*, **20**, (in press).

Torquato, S., Lu, B. and Rubinstein J., "Nearest-Neighbor Distribution Functions in Many-Body Systems," *Phys. Rev. A*, **41**, 2059 (1990).

Torquato, S. and Avellaneda, M., "Diffusion and Reaction in Heterogeneous Media: Pore Size Distribution, Relaxation Times, and Mean Survival Time," *J. Chem. Phys.*, **95**, 6477 (1991).